Check for
updates

Insights Into Chemical Reactions at the Beginning of the Universe: From HeH$^+$ to H$_3^+$

Soumya Ranjan Dash[1†], Tamal Das[1,2†] and Kumar Vanka[1,2]*

[1]Physical and Materials Chemistry Division, CSIR-National Chemical Laboratory (CSIR-NCL), Pune, India, [2]Academy of Scientific and Innovative Research (AcSIR), Ghaziabad, India

At the dawn of the Universe, the ions of the light elements produced in the Big Bang nucleosynthesis recombined with each other. In our present study, we have tried to mimic the conditions in the early Universe to show how the recombination process would have led to the formation of the first ever formed diatomic species of the Universe: HeH$^+$, as well as the subsequent processes that would have led to the formation of the simplest triatomic species: H$_3^+$. We have also studied some special cases: higher positive charge with fewer number of hydrogen atoms in a dense atmosphere, and the formation of unusual and interesting linear, dicationic He chains beginning from light elements He and H in a positively charged atmosphere. For all the simulations, the *ab initio* nanoreactor (*AINR*) dynamics method has been employed.

Keywords: density functional theory, ab initio molecular dynamics, ab initio nanoreactor, origin of molecules in the universe, the earliest lewis acid

INTRODUCTION

The way the Universe, and all the elements, came into being is one of the fascinating questions of science. Attempts to answer this question has led to the Big Bang theory, and an understanding of the primeval Universe and the entities that it was made up of (Meyer, 2008). Further advancement of science and technology has led to greater understanding, which led NASA's Stratospheric Observatory for Infrared Astronomy (SOFIA) to the detection of HeH$^+$ in the planetary nebula NGC 7027, the first molecule formed after the Big Bang (Güsten et al., 2019), 94 years after its discovery in the laboratory in 1925 (Hogness and Lunn, 1925).

As the first molecule, the significance of the role of HeH$^+$ in the evolution of other species cannot be overstated. One of these species, and perhaps the most important, is the simplest polyatomic molecule H$_3^+$, which has always intrigued researchers ever since its discovery in 1911 by J. J. Thomson (Sir Thomson, 1911). However, the importance H$_3^+$ in astrochemistry was realized only after it was detected on Jupiter in the 1980s (Oka, 1980; Drossart et al., 1989). High abundance of H$_3^+$ in the Universe and its ability to donate a proton established this triatomic cation as the interstellar acid of utmost importance for many extra-terrestrial reactions (Watson, 1973; Oka, 2013; Olah et al., 2016; Pelley, 2019). While there are many reports of H$_3^+$ formation from doubly ionized organic molecules (Townsend et al., 2004; De et al., 2006; Okino et al., 2006; Kushawaha and Bapat, 2008; Mebel and Bandrauk, 2008; Nakai et al., 2013; Ando et al., 2018;

Abbreviations: AIMD, *Ab initio* molecular dynamics; AINR, *Ab initio* nano reactor; DFT, Density functional theory.

GRAPHICAL ABSTRACT |

Ekanayake et al., 2018; Palaudoux and Hochlaf, 2019), our focus is on its origin and the role played by HeH$^+$ on its formation.

H_3^+ formation was first reported to occur primarily from the combination of H_2^+ and H_2, where H_2^+ would be formed from the ionization of H_2 (Sir Thomson, 1912; Oka, 2013). There are other reports which state that H_2^+ is more likely to be formed from the combination of HeH$^+$ and H (Bovino et al., 2011; Razio, 2014; Esposito et al., 2015; Fortenberry, 2019; González-Lezana et al., 2019). At the same time, the possibility of HeH$^+$ combining with H_2 to produce H_3^+ cannot be overlooked (McLaughlin and Thompson, 1973). Thus, many factors can influence the origin of H_3^+, but there have not been any conclusive studies yet.

In this work, we have employed the *ab initio* nanoreactor (AINR) method to carry out full quantum mechanical molecular dynamics (MD) simulations on systems containing atoms/ions of helium and hydrogen, and have obtained reaction profiles by varying their mixture ratio and the charge. The *AINR* method, developed by Martinez and co-workers, allows the determination of new reaction pathways and products, without the need of controlling the chemical system (Zimmerman, 2013; Rappoport et al., 2014; Wang et al., 2014). Our primary goal was to gain insight into the formation of different species from the combination of He and H in the presence of a positively charged atmosphere, as well as their further dissociation and recombination. As the Results and Discussion section will show, our studies provide interesting new insights into HeH$^+$ formation, and shed light on various short-lived intermediates that could have formed *en route* to obtaining H_3^+– the stable species that was known to exist in the early Universe (Oka, 2013).

COMPUTATIONAL METHODS

Ab Initio Molecular Dynamics Simulations
The AIMD simulations were performed with the TeraChem 1.9 (Ufimtsev and Martínez, 2008a; Ufimtsev and Martínez, 2008b; Ufimtsev and Martinez, 2009a; Ufimtsev and Martinez, 2009b; Ufimtsev et al., 2011; Isborn et al., 2011; Titov et al.,

2013) software package using the Hartree−Fock (HF) (Fischer, 1987) electronic wave function and the 6–311 g (Binkley et al., 1980) Gaussian basis set, to calculate the Born−Oppenheimer potential energy surface. This method has been implemented in TeraChem by Martinez and co-workers. This approach was deemed acceptable because the HF method is well-known for predicting chemically reasonable structures (Feller and Peterson, 1998). Also, it should be noted that HF was not employed to determine the thermodynamics of the reactions: its only role was in the discovery process. This was also the approach employed by Martinez and co-workers in their original *AINR* paper (employing HF/3–21 g), where they replicated the results obtained from the Urey−Miller experiment, as well as from the interaction of acetylene molecules. The same method (HF) was also employed by us in our previous report (Das et al., 2019) on reaction pathways leading to the formation of precursors of RNA and sugars. Electrostatic interactions were treated using two of the most common methods: the residue-based cutoff and particle mesh Ewald (PME). The PME method has been chosen because it takes care of long-range electrostatic interactions and is the most widely used approach.

The results were obtained from the *AINR* simulations by varying both the He to H ratio, as well as the positive charge of the system. Each simulation was repeated thrice. The system was constrained in a spherical boundary of 4.0 and 2.0 Å radii, so that the atoms resided in a space that alternated between the volumes created by these two radii, and collided with each other. Each *AINR* dynamics was evolved upto 15 ps, with a time step of 0.5 fs.

Newton's equations of motion were calculated using Langevin dynamics, with an equilibrium temperature of 1,000.0 K (also the starting temperature of the dynamics). We have used this high temperature in order to increase the average kinetic energy of the reactants and for faster dynamics (Novotný et al., 2019). We have employed the augmented direct inversion in the iterative subspace (ADIIS) algorithm (Hu and Yang, 2010) available in TeraChem as an alternative tool for self-consistent field calculations at each AIMD step in

which the default DIIS algorithm (Pulay, 1980) failed to converge. The nanoreactor simulations employ a virtual piston by fluctuating the radius of a spherical boundary, which allows the continuous expansion and compression of the system, thus artificially changing the pressure and the density for the collision cycles, which is necessary for the molecules to collide and also increases the rate of the reactions. Spherical boundary conditions (details in the ESI) were applied to prevent the molecules from flying away, a phenomenon known as the "evaporation" event. For more details, please check the original paper on the *AINR* by Martinez and co-workers (Wang et al., 2014).

The mechanistic pathways obtained from the *AINR* simulations were then analyzed with full quantum mechanical (QM) calculations. All the structures were optimized with coupled cluster singles doubles (CCSD) (Grotendorst et al., 2006) and with the 6–311++G (d,*p*) (McLean and Chandler, 1980) basis set. The Gaussian09 software (Frisch et al., 2009) was employed for the thermodynamic calculations. The complete solution of the H_3^+ problem requires the consideration of relativistic effects, nuclear motion, and breakdown of the Born-Oppenheimer (B-O) approximation (both adiabatic and non-adiabatic) (Miller et al., 2020). Recent studies have shown that relativistic effects for H_3^+ are quite negligible (Cencek et al., 1998; Bachorz et al., 2009). Issues of breakdown of the B-O approximation become relevant when considering transition frequencies of H_3^+, i.e., in spectroscopic studies. Since the current work is focused on understanding the possible chemical reactivity and thermochemistry of HeH^+ and H^+, leading eventually to H_3^+ formation, the current studies, done within the B-O approximation, are appropriate.

RESULTS AND DISCUSSIONS

In this section, we will briefly describe the formation of H_3^+ in the *AINR via* different short lived intermediates. We have taken a fixed composition of the He and H mixture and varied the overall positive charge density of the system (as shown in **Tables 1**, **2**). During the simulations in each case, it was seen that HeH^+ was formed at the very beginning of the dynamics as the first molecular species. In our first set of simulations, we have taken a homogeneous mixture of 30 atoms each of H and He. The *AINR* makes them collide with each other at a temperature of 1,000.0 K. The simulation with no positive charge in the system does not produce any intermediates and H_3^+ at all throughout the dynamics. This led us to consider the possibility that a more appropriate set-up would include a positively charged system, which would mimic the collisions between the ionized state of the helium and hydrogen atoms present at the beginning of Universe (Oka, 2013). A positively charged environment for the formation of H_3^+ had also been considered by many previous reports, while investigating its origin from different organic molecules (Pilling et al., 2007). Therefore, we have varied the positive charge of the system by even numbers (**Table 1**) during the *AINR* dynamics. As the dynamics progressed, various short lived species such as He_2^{2+}, He_3^{2+} and He_2H^+ (snapshots shown in the **Supplementary Figures S1–S5** in the Supporting Information (ESI) file) were seen to have formed in almost every simulation, though their time of appearance was different in each case. It was also observed that with the increase of the positive charge of the system, the formation of H_3^+ ions also increased, up to a point. The number of H_3^+ ions generated was equal to the positive charge in the system, up to a charge of +6 (see **Table 1**).

TABLE 1 | *AINR* simulations with 30 He atoms and 30 H atoms: different entries represent the variation of the total positive charge of the system–by even numbers.

Total charge	First molecule	Intermediate species	Dominant end molecule	No. of H_3^+
0	-	-	-	-
2	HeH^+	He_2^{2+}, He_3^{2+}, He_2H^+, H^+, H_2	H_3^+	2
4	HeH^+	He_2^{2+}, He_2H^+, H^+, H_2	H_3^+	4
6	HeH^+	He_2^{2+}, He_3^{2+}, He_2H^+, H^+, H_2	H_3^+	6
8	HeH^+	He_2^{2+}, He_3^{2+}, He_2H^+, H^+, H_2	H_3^+	7
10	HeH^+	He_2^{2+}, He_3^{2+}, He_2H^+, H^+, H_2	H_3^+	7
20	HeH^+	He_2^{2+}, He_2H^+, H^+, H_2	H_3^+	5

TABLE 2 | *AINR* simulations with 30 He atoms and 29 H atoms: different entries represent the variation of the total positive charge of the system–by odd numbers.

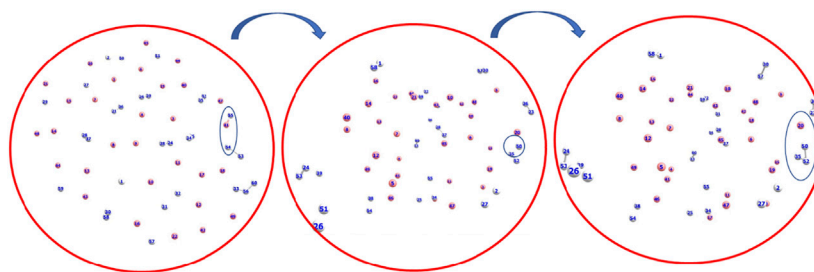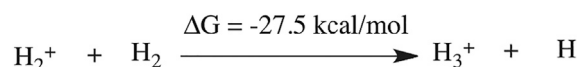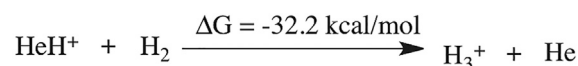| Total charge	First molecule	Intermediate species	Dominant end molecule	No. of H_3^+
0	-	-	-	-
1	HeH^+	He_2H^+, H^+, H_2	H_3^+	1
3	HeH^+	He_2^{2+}, He_2H^+, H^+, H_2	H_3^+	3
5	HeH^+	He_2^{2+}, He_2H^+, H^+, H_2	H_3^+	5
7	HeH^+	He_2^{2+}, He_3^{2+}, He_2H^+, H^+, H_2	H_3^+	6
9	HeH^+	He_2^{2+}, He_3^{2+}, He_2H^+, H^+, H_2	H_3^+	7
11	HeH^+	He_2^{2+}, He_2H^+, H^+, H_2	H_3^+	7
21	HeH^+	He_2^{2+}, He_2H^+, H^+, H_2	H_3^+, HeH^+	4

FIGURE 1 | Snapshots of *AINR* simulations showing the progress of the dynamics starting from atomic He and H, leading toward the formation of H_3^+ from HeH^+ and dihydrogen. HeH^+ was seen to be formed very early–near the beginning of the dynamics (Color: He - peach, H - white).

$$HeH^+ \; + \; H_2 \; \xrightarrow{\Delta G = -32.2 \text{ kcal/mol}} \; H_3^+ \; + \; He$$

$$H_2^+ \; + \; H_2 \; \xrightarrow{\Delta G = -27.5 \text{ kcal/mol}} \; H_3^+ \; + \; H$$

SCHEME 1 | Thermodynamics of H_3^+ formation.

However, upon further increase in the positive charge of the system beyond six–to eight or ten, the number of H_3^+ ions formed was not seen to be equal to the total positive charge of the system. Instead of H_3^+, the remaining positive charge of the system was balanced by H^+ or, in some cases, HeH^+. As shown in **Table 1**, in case of a positive charge of 10 and after 250 fs, we observed only seven H_3^+ ions remaining with three H^+, which balanced the total charge of the system. The natural population analysis (NPA), or the formal charge analyzed data for all the atoms in several snapshots, has been shown in **Supplementary Tables S1–S4** in the ESI.

Similarly, in another set of MD simulations, we have taken 29 H with 30 He atoms and varied the overall charge of the system by an odd number: one, three, five and so on. These observations have been shown in **Table 2**. We have observed a similar trend for the formation of H_3^+ as the only end product up to a certain limit (here, the value is 5) of positive charge and beyond that, the total charge of the system was seen to be balanced by the sum of H_3^+, H^+ and HeH^+, as seen in the previous section when the positive charge was varied by even numbers.

In short, we can say that in all the cases of AINR dynamics studied, the formation of HeH^+ as the first molecule was observed. However, upon varying the total positive charge of the whole system, several short-lived species (He_2H^+, He_3^{2+}, He_2^{2+}) were observed (**Tables 1, 2**) after HeH^+ formation. At the end of the simulation, H_3^+ and H_2 were found to be the only stable species left in the reaction mixture.

The Timescale of Formation of H_3^+ and Other Short Lived Molecules

The formation timescale of different short lived species, along with the stable H_3^+, has been observed from femtosecond *AINR* simulations. In each and every simulation, HeH^+, which has been proposed to be the first formed molecule, was seen to be formed soon after the beginning of the dynamics. The time of appearance

of HeH^+ was within 15 fs timesteps. Subsequently, other short lived species (He_2H^+, He_3^{2+}, He_2^{2+}) were formed within the timescale of 0.1 ps (shown in **Table 3**). The observed timescale for the existence of such transient species is around 5–10 fs. Once these molecules were formed, they quickly dissociated and this ultimately led to the formation of H_3^+, which was observed for every case. From the AINR dynamics, we have analyzed the data and found two pathways for the formation of H_3^+, starting from He and H in atomic states within the positively charge atmosphere. Both of the pathways involved the well-known roaming hydrogen mechanism (Townsend et al., 2004; Nakai et al., 2013; Palaudoux and Hochlaf, 2019). An mp4 file (**Supplementary Movie S1**) of a movie made of a part of an *AINR* simulation is included in the ESI. The most feasible pathway for H_3^+ formation is the abstraction of a proton from the first molecule HeH^+ by the roaming dihydrogen (shown in **Figure 1**).

The thermodynamics for this step has been calculated to be -32.2 kcal/mol (shown in **Scheme 1**). In another mechanistic pathway, there is no involvement of HeH^+. Instead of HeH^+, the proton abstraction occurs from a mono-cationic dihydrogen molecule by the roaming dihydrogen. This process is thermodynamically favourable by 27.5 kcal/mol.

The total number of H_3^+ molecules formed was also found to be directly correlated with the total charge of the system, as well as

TABLE 3 | Time (in fs) of the first appearance of different species.

Total charge	HeH^+	He_2H^+	He_2^{2+}	He_3^{2+}	H_3^+
0	-	-	-	-	-
2	4.5	11.0	10.0	25.5	27.0
4	9.0	25.5	19.5	80.0	45.0
6	5.0	12.5	16.0	49.5	9.0
8	4.0	12.5	22.5	53.0	8.0
10	5.5	18.0	14.0	19.0	7.0
20	4.0	26.5	14.5	22.0	9.0

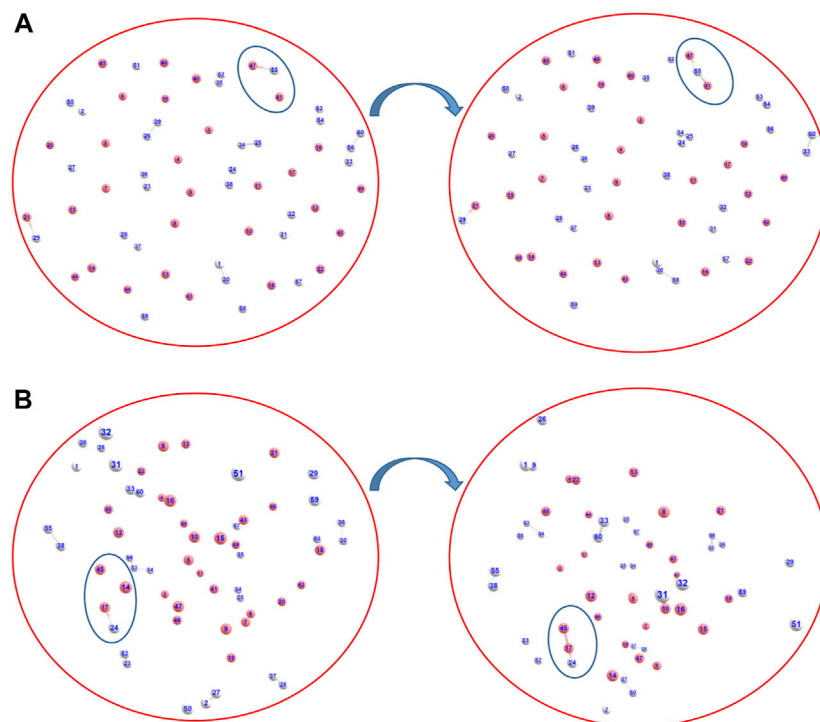**FIGURE 2 |** Snapshots of *AINR* simulations revealing the pathway toward the making of He₂H⁺, in the form of **(A)** [He-H-He]⁺ and **(B)** [He-He-H]⁺ (Color: He - peach, H - white).

the number of He and H atoms taken. Greater charge in the system yielded more short-lived species during the simulations. Most of the intermediate species were found to be formed within 100 fs (**Table 3**) and they were found to exist for only about 5–10 fs during the *AINR* simulations.

Since it has been postulated that different ratios of helium to hydrogen atoms could have existed in the early Universe (Meyer, 2008), we have further performed *AINR* dynamics with a 1:3 ratio of helium to hydrogen atoms and varied the total positive charge of the system (see **Table 4**). Furthermore, in order to investigate the effect of temperature on cosmic reionization (Novotný et al., 2019), we have also carried out *AINR* simulations while varying the temperature (**Table 5**), with a 1:3 ratio of He:H and a fixed positive charge (8⁺). In all such simulations, we have observed trends similar to those discussed in the previous sections, like the formation of HeH⁺ as the first molecule and the subsequent

formation of transient species (He₂H⁺, He₃²⁺, He₂²⁺), leading eventually to H₃⁺ formation.

We have also addressed the speculation on the exact nature of the formed ion He₂H⁺: whether it was formed as [He-H-He]⁺ or as [He-He-H]⁺ (Kim and Lee, 1999), *via AINR* dynamics followed by static CCSD calculations. As shown in **Figures 2A,B**, two different routes leading to the formation of [He-H-He]⁺ and [He-He-H]⁺ were observed during the simulations, generated from the collision of HeH⁺ and He. The thermodynamics was evaluated and it was found that the formation of the [He-H-He]⁺ species was exergonic by 32.3 kcal/mol, whereas the formation of [He-He-H]⁺ was only favourable by 4.5 kcal/mol. In other words, our calculations indicate that He₂H⁺ would have formed predominantly as [He-H-He]⁺ rather than [He-He-H]⁺.

In another set of simulations, we have taken a different ratio of helium to dihydrogen and simultaneously varied the total charge

TABLE 4 | Time of occurrence (in fs) of different species from the *AINR* simulation of 1: 3 ratio of helium to hydrogen while varying total positive charge of the system.

Total charge	HeH⁺	He₂H⁺	He₂²⁺	He₃²⁺	H₃⁺
0	-	-	-	-	-
4	5.0	74.5	14.0	24.0	12.5
6	9.5	15.5	12.0	27.0	17.0
8	6.0	54.0	15.0	19.5	21.5
10	10.0	16.0	14.5	30.0	19.0
12	6.5	70.5	16.0	23.0	23.0

TABLE 5 | Time of occurrence (in fs) of different species from the *AINR* simulation of a 1: 3 ratio of helium to hydrogen while varying the temperature, with a fixed total positive charge of system (8⁺).

Temperature (K)	HeH⁺	He₂H⁺	He₂²⁺	He₃²⁺	H₃⁺
3,300	3.0	24.5	10.0	26.0	5.5
2,500	8.5	27.0	14.0	18.0	63.0
2,000	7.0	22.0	16.0	19.0	25.0
1,500	7.0	14.0	11.5	17.0	60.0
1,000	6.0	54.0	15.0	19.5	21.5
500	8.0	16.0	15.0	20.5	47.0

of the system. In these cases, due to the high charge density, the dihydrogen quickly dissociated into a proton and atomic hydrogen. Here too, we have observed similar trends: 1) HeH$^+$ is the first molecule to be formed, followed by 2) the formation of other short lived species, leading to H$_3^+$, which remained at the end, along with one or two molecules of HeH$^+$ (shown in **Table 5**). For the case of 20 He and five H$_2$ having a total of eight positive charge in the system, for instance, we observed that after a few collisions, there was still one HeH$^+$ molecule present along with one H$_3^+$ and that they were in equilibrium with each other, due to the instantaneous proton transfer between HeH$^+$ and H$_2$. Similar trends were observed for other simulations where the total positive charge of the system was high (in our simulation conditions, the values were ≥16). It is worth mentioning that in this high positive charge atmosphere with comparatively low H atom density, the number of H$_3^+$ that survived after the collisions was either one or two, depending upon the ratio of He to H$_2$ (shown in **Table 6**). Also, due to the very high positive charge density and high temperature (1,000.0 K) the movement of the light H$^+$ ions was seen to be extremely fast and they repelled each other, going far away. This reduced the propensity toward the formation of H$_3^+$ in such simulations.

Formation of Unique Dicationic He Chains

Previously, there have been some reports (Marinetti et al., 2008; Oleksy et al., 2010) with regard to the formation of mono-cationic He ion clusters. Our current *AINR* based dynamics study reveals that there is a possibility of the formation of a dicationic helium chain of up to five He atoms: He$_3^{2+}$, He$_4^{2+}$ and He$_5^{2+}$. This interesting result was obtained when we took a homogeneous mixture of H and He (15 atoms each) in the AINR, with an overall positive charge of 20 for the system. After a certain amount of time had elapsed (1 ps), we observed that a chain like structure had formed comprising of up to five helium atoms (shown in **Figure 3**).

An mp4 file (**Supplementary Movie S2**) of a movie made of a part of such an *AINR* simulation is included in the ESI. We have taken snapshots during the dynamics and carried out natural population analysis (NPA), in order to calculate the charge on the

TABLE 6 | Different ratios of He to dihydrogen while varying the total positive charge of the system.

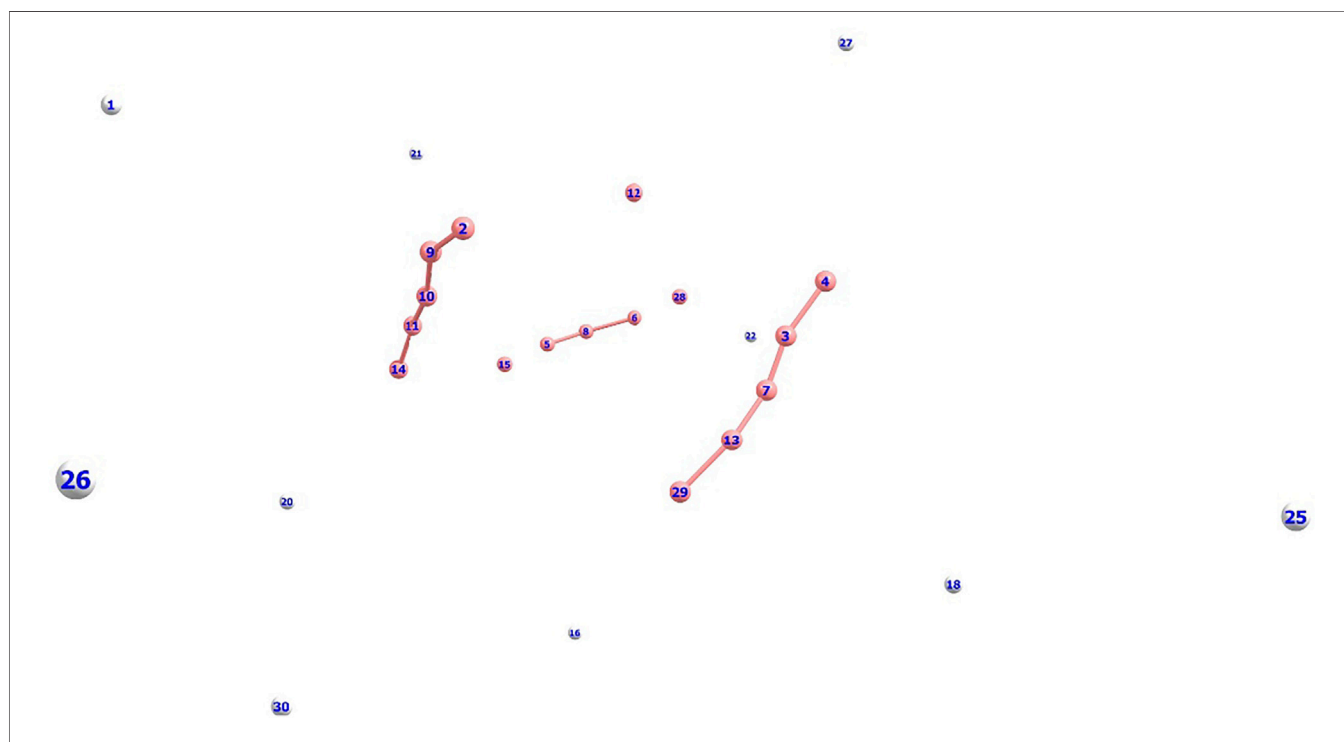| No. of He	No. of H$_2$	Total charge	First molecule	Intermediate species	Dominating end molecule	No. of H$_3^+$
20	5	8	HeH$^+$	He$_2^{2+}$, H$^+$	HeH$^+$, H$_3^+$	1
30	10	16	HeH$^+$	He$_2^{2+}$, He$_3^{2+}$, He$_2$H$^+$, H$^+$	HeH$^+$, H$_3^+$	1
30	15	24	HeH$^+$	He$_2^{2+}$, He$_2$H$^+$, H$^+$	HeH$^+$, H$_3^+$	1
30	15	26	HeH$^+$	He$_2^{2+}$, He$_2$H$^+$, H$^+$	HeH$^+$, H$_3^+$	1
15	10	8	HeH$^+$	He$_2^{2+}$, He$_2$H$^+$, H$^+$	H$_3^+$	4
30	15	20	HeH$^+$	He$_2^{2+}$, He$_3^{2+}$, He$_2$H$^+$, H$^+$	HeH$^+$, H$_3^+$	4

FIGURE 3 | Dicationic He chain formation during an *AINR* simulation of 15 H and 15 He atoms, with an overall positive charge of 20 (Color: He - peach, H - white).
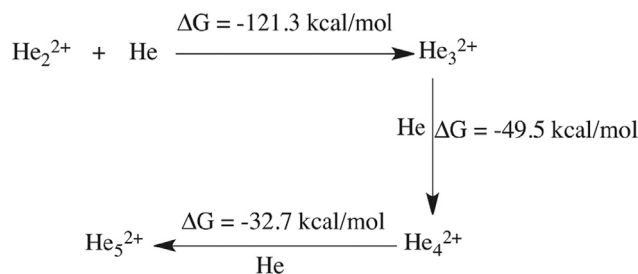
SCHEME 2 | Thermodynamics of helium chain formation (up to He_5^{2+}).

He atoms in the formed linear chain. From the NPA charge analysis (shown in **Supplementay Table S6** in the ESI), it has been confirmed that all the formed He chains (He_3^{2+}, He_4^{2+}, He_5^{2+}) were dicationic in nature. For further confirmation of the stability of these dicationic He chains, we have done thermodynamics calculations for the formation of the He chain starting from He_2^{2+} (shown in **Scheme 2**). The Gibbs free energy values suggest that the formation of the dicationic helium chain up to He_5^{2+} is favourable, but further formation of He_6^{2+} is thermodynamically not feasible. For this reason, we did not observe any He chain beyond five He atoms in our *AINR* simulations.

CONCLUSION

In our current work, we have tried to shed light on the chemical reactions that might have taken place at the beginning of the Universe. We have focused on how, at the very beginning, simple molecules came into being after the Big Bang. We have investigated how He and H atoms, which were the first atoms formed, collided with each other in a positively charged atmosphere. This has been done by using a fresh computational approach–by employing the *ab initio* nanoreactor (*AINR*). The simulations reveal the presence of unique dicationic helium chains of up to five atoms, which should act as a fillip for investigating the possibility of the presence of such species in helium clusters, which have received attention both from experimental and theoretical studies (Bieske and Dopfer, 2000; Marinetti et al., 2008; Oleksy et al., 2010). Our studies also confirm that HeH^+ was indeed the first molecule to be formed and that it played a vital role in the origin of H_3^+. The preservation of H_3^+, as a relatively stable species, in each of the simulations after every collision cycle, also explains the high abundance of H_3^+ in the early Universe. As such, our work provides interesting computational insights into the origin of unique and interesting molecules at the dawn of the Universe.

REFERENCES

Ando, T., Shimamoto, A., Miura, S., Iwasaki, A., Nakai, K., and Yamanouchi, K. (2018). Coherent Vibrations in Methanol Cation Probed by Periodic H_3^+ Ejection after Double Ionization. *Comm. Chem.* 1, 7. doi:10.1038/s42004-017-0006-7

DATA AVAILABILITY STATEMENT

The original contributions presented in the study are included in the article/**Supplementary Material**, further inquiries can be directed to the corresponding author.

AUTHOR CONTRIBUTIONS

SD and TD have carried out the research work and written the manuscript, with the guidance and supervision of KV.

FUNDING

ACKNOWLEDGMENTS

SUPPLEMENTARY MATERIAL

The Supplementary Material for this article can be found online at: https://www.frontiersin.org/articles/10.3389/fchem.2021.679750/full#supplementary-material

Bachorz, R. A., Cencek, W., Jaquet, R., and Komasa, J. (2009). Rovibrational Energy Levels of H 3+ with Energies above the Barrier to Linearity. *J. Chem. Phys.* 131, 024105. doi:10.1063/1.3167795

Bieske, E. J., and Dopfer, O. (2000). High-resolution Spectroscopy of Cluster Ions. *Chem. Rev.* 100, 3963–3998. doi:10.1021/cr990064w

Binkley, J. S., Pople, J. A., and Hehre, W. J. (1980). Self-consistent Molecular Orbital Methods. 21. Small Split-Valence Basis Sets for

First-Row Elements. *J. Am. Chem. Soc.* 102 (3), 939–947. doi:10.1021/ja00523a008

Bovino, S., Gianturco, F. A., and Tacconi, M. (2011). Chemical Destruction of Rotationally "Hot" HeH$^+$: Quantum Cross Sections and Mechanisms of its Reaction with H. *Chem. Phys. Lett.* 554, 47–52. doi:10.1016/j.cplett.2012.10.027

Cencek, W., Rychlewski, J., Jaquet, R., and Kutzelnigg, W. (1998). Sub-microhartree Accuracy Potential Energy Surface for H3+ Including Adiabatic and Relativistic Effects. I. Calculation of the Potential Points. *J. Chem. Phys.* 108, 2831–2836. doi:10.1063/1.4757027

Das, T., Ghule, S., and Vanka, K. (2019). Insights into the Origin of Life: Did it Begin from HCN and H2O? *ACS Cent. Sci.* 5 (9), 1532–1540. doi:10.1021/acscentsci.9b00520

De, S., Rajput, J., Roy, A., Ghosh, P. N., and Safvan, C. P. (2006). Formation of H$_3^+$ Due to Intramolecular Bond Rearrangement in Doubly Charged Methanol. *Phys. Rev. Lett.* 97, 1–4. doi:10.1103/physrevlett.97.213201

Drossart, P., Maillard, J.-P., Caldwell, J., Kim, S. J., Watson, J. K. G., Majewski, W. A., et al. (1989). Detection of H3+ on Jupiter. *Nature* 340, 539–541. doi:10.1038/340539a0

Ekanayake, N., Severt, T., Nairat, M., Weingartz, N. P., Farris, B. M., Kaderiya, B., et al. (2018). H$_2$ Roaming Chemistry and the Formation of H$_3$ $^+$ from Organic Molecules in Strong Laser Fields. *Nat. Comm* 9, 5186. doi:10.1038/s41467-018-07577-0

Esposito, F., Coppola, C. M., and De Fazio, D. (2015). Complementarity between Quantum and Classical Mechanics in Chemical Modeling. The H + HeH+ → H2+ + He Reaction: A Rigorous Test for Reaction Dynamics Methods. *J. Phys. Chem. A.* 119 (51), 12615–12626. doi:10.1021/acs.jpca.5b09660

Feller, D., and Peterson, K. A. (1998). An Examination of Intrinsic Errors in Electronic Structure Methods Using the Environmental Molecular Sciences Laboratory Computational Results Database and the Gaussian-2 Set. *J. Chem. Phys.* 108, 154–176. doi:10.1063/1.475370

Fischer, C. F. (1987). General Hartree-Fock Program. *Comput. Phys. Comm.* 4, 355–365. doi:10.1016/0010-4655(87)90053-1

Fortenberry, R. C. (2019). The Oldest Molecular Ancestor Finally Brought into the Light. *Chem* 5, 1012–1030. doi:10.1016/j.chempr.2019.04.016

Frisch, M. J., Trucks, G. W., Schlegel, H. B., Scuseria, G. E., Robb, M. A., Cheeseman, J. R., et al. (2009). *Gaussian 09, Revision A.01*. Wallingford CT: Gaussian, Inc.

González-Lezana, T., Bossion, D., Scribano, Y., Bhowmick, S., and Suleimanov, Y. V. (2019). Dynamics of H + HeH+(v = 0, J = 0) → H2+ + He: Insight on the Possible Complex-Forming Behavior of the Reaction. *J. Phys. Chem. A.* 123 (49), 10480–10489. doi:10.1021/acs.jpca.9b06122

Grotendorst, J., Blugel, S., and Marx, D. (2006). Beyond Hartree-Fock: MP2 and Coupled-Cluster Methods for Large Systems. *Comput. Nanoscience* 31, 245–278.

Güsten, R., Wiesemeyer, H., Neufeld, D., Menten, K. M., Graf, U. U., Jacobs, K., et al. (2019). Astrophysical Detection of the Helium Hydride Ion HeH+. *Nature* 568, 357–359. doi:10.1038/s41586-019-1090-x

Hogness, T. R., and Lunn, E. G. (1925). The Ionization of Hydrogen by Electron Impact as Interpreted by Positive Ray Analysis. *Phys. Rev.* 26, 44–55. doi:10.1103/physrev.26.44

Hu, X., and Yang, W. (2010). Accelerating Self-Consistent Field Convergence with the Augmented Roothaan−Hall Energy Function. *J. Chem. Phys.* 132, 054109. doi:10.1063/1.3304922

Isborn, C. M., Luehr, N., Ufimtsev, I. S., and Martínez, T. J. (2011). Excited-State Electronic Structure with Configuration Interaction Singles and Tamm-Dancoff Time-dependent Density Functional Theory on Graphical Processing Units. *J. Chem. Theor. Comput.* 7 (6), 1814–1823. doi:10.1021/ct200030k

Kim, S. T., and Lee, J. S. (1999). Ab Initio study of He2H+ and Ne2H+: Accurate Structure and Energetics. *J. Chem. Phys.* 110, 4413–4418. doi:10.1063/1.478324

Kushawaha, R. K., and Bapat, B. (2008). Fragmentation Dynamics of the Methanol Dication. *Chem. Phys. Lett.* 463, 42–46. doi:10.1016/j.cplett.2008.08.019

Marinetti, F., Bodo, E., Gianturco, F. A., and Yurtsever, E. (2008). Energetics and Structures of Charged Helium Clusters: Comparing Stabilities of Dimer and Trimer Cationic Cores. *ChemPhysChem* 9, 2618–2624. doi:10.1002/cphc.200800457

McLaughlin, D. R., and Thompson, D. L. (1973). Ab Initio dynamics: HeH+ + H2 → He + H3+ (C 2v) Classical Trajectories Using a Quantum Mechanical Potential-energy Surface. *J. Chem. Phys.* 59, 4393–4405. doi:10.1063/1.1680637

McLean, A. D., and Chandler, G. S. (1980). Contracted Gaussian Basis Sets for Molecular Calculations. I. Second Row Atoms, Z=11-18. *J. Chem. Phys.* 72, 5639–5648. doi:10.1063/1.438980

Mebel, A. M., and Bandrauk, A. D. (2008). Theoretical Study of Unimolecular Decomposition of Allene Cations. *J. Chem. Phys.* 129, 224311. doi:10.1063/1.3037204

Meyer, B. S. (2008). Origin of the Elements: Nucleosynthesis in Stars. *ACS Symp. Ser.* 981 (3), 39–60. doi:10.1021/bk-2008-0981.ch003

Miller, S., Tennyson, J., Geballe, T. R., and Stallard, T. (2020). Thirty Years of H$_3^+$ Astronomy. *Rev. Mod. Phys.* 92, 035003. doi:10.1103/revmodphys.92.035003

Nakai, K., Kato, T., Kono, H., and Yamanouchi, K. (2013). Communication: Long-Lived Neutral H$_2$ in Hydrogen Migration within Methanol Dication. *J. Chem. Phys.* 139, 1–5. doi:10.1063/1.4830397

Novotný, O., Wilhelm, P., Paul, D., Kálosi, Á., Saurabh, S., Becker, A., et al. (2019). Quantum-state-selective Electron Recombination Studies Suggest Enhanced Abundance of Primordial HeH+. *Science* 365, 676–679. doi:10.1126/science.aax5921

Oka, T. (2013). Interstellar H3+. *Chem. Rev.* 113, 8738–8761. doi:10.1021/cr400266w

Oka, T. (1980). Observation of the Infrared Spectrum of H3+. *Phys. Rev. Lett.* 45 (7), 531–534. doi:10.1103/physrevlett.45.531

Okino, T., Furukawa, Y., Liu, P., Ichikawa, T., Itakura, R., Hoshina, K., et al. (2006). Coincidence Momentum Imaging of Ejection of Hydrogen Molecular Ions from Methanol in Intense Laser Fields. *Chem. Phys. Lett.* 419, 223–227. doi:10.1016/j.cplett.2005.11.059

Olah, G. A., Mathew, T., and Prakash, G. K. S. (2016). Relevance and Significance of Extraterrestrial Abiological Hydrocarbon Chemistry. *J. Am. Chem. Soc.* 138 (22), 6905–6911. doi:10.1021/jacs.6b03136

Oleksy, K., Karlický, F., and Kalus, R. (2010). Structures and Energetics of Helium Cluster Cations: Equilibrium Geometries Revisited through the Genetic Algorithm Approach. *J. Chem. Phys.* 133, 164314. doi:10.1063/1.3489346

Palaudoux, J., and Hochlaf, M. (2019). Formation of H3+ through Chloromethane Dication Fragmentation. *ACS Earth Space Chem.* 3 (6), 980–985. doi:10.1021/acsearthspacechem.9b00045

Pelley, J. (2019). Probing the Universe with H$_3^+$. *ACS Cent. Sci.* 5 (5), 741–744. doi:10.1021/acscentsci.9b00555

Pilling, S., Andrade, D. P. P., Neves, R., Ferreira-Rodrigues, A. M., Santos, A. C. F., and Boechat-Roberty, H. M. (2007). Production of H+3 via Photodissociation of Organic Molecules in Interstellar Clouds. *Mon. Not. R. Astron. Soc.* 375 (4), 1488–1494. doi:10.1111/j.1365-2966.2006.11415.x

Pulay, P. (1980). Convergence Acceleration of Iterative Sequences. The Case of SCF Iteration. *Chem. Phys. Lett.* 73, 393–398. doi:10.1016/0009-2614(80)80396-4

Rappoport, D., Galvin, C. J., Zubarev, D. Y., and Aspuru-Guzik, A. (2014). Complex Chemical Reaction Networks from Heuristics-Aided Quantum Chemistry. *J. Chem. Theor. Comput.* 10, 897–907. doi:10.1021/ct401004r

Razio, D. D. (2014). The H + HeH$^+$ → He + H$_2^+$ Reaction from the Ultra-cold Regime to the Three-Body Breakup: Exact Quantum Mechanical Integral Cross Sections and Rate Constants. *Phys. Chem. Chem. Phys.* 16, 11662–11672. doi:10.1039/c4cp00502c

Sir Thomson, J. J. (1911). Rays of Positive Electricity. *Philos. Mag.* 6 (21), 225. doi:10.1080/14786440208637024

Sir Thomson, J. J. (1912). Rays of Positive Electricity. *Philos. Mag.* 6 (24), 209. doi:10.1080/14786440808637325

Titov, A. V., Ufimtsev, I. S., Luehr, N., and Martinez, T. J. (2013). Generating Efficient Quantum Chemistry Codes for Novel Architectures. *J. Chem. Theor. Comput.* 9 (1), 213–221. doi:10.1021/ct300321a

Townsend, D., Lahankar, S. A., Lee, S. K., Chambreau, S. D., Suits, A. G., Zang, X., et al. (2004). The Roaming Atom: Straying from the Reaction Path in Formaldehyde Decomposition. *Science* 306, 1158–1161. doi:10.1126/science.1104386

Ufimtsev, I. S., Luehr, N., and Martinez, T. J. (2011). Charge Transfer and Polarization in Solvated Proteins from *Ab Initio* Molecular Dynamics. *J. Phys. Chem. Lett.* 2 (14), 1789–1793. doi:10.1021/jz200697c

Ufimtsev, I. S., and Martínez, T. J. (2008a). Graphical Processing Units for Quantum Chemistry. *Comput. Sci. Eng.* 10, 26–34. doi:10.1109/mcse.2008.148

Ufimtsev, I. S., and Martínez, T. J. (2008b). Quantum Chemistry on Graphical Processing Units. 1. Strategies for Two-Electron Integral Evaluation. *J. Chem. Theor. Comput.* 4 (2). 222–231.doi:10.1021/ct700268q

Ufimtsev, I. S., and Martinez, T. J. (2009a). Quantum Chemistry on Graphical Processing Units. 2. Direct Self-Consistent-Field Implementation. *J. Chem. Theor. Comput.* 5 (4), 1004–1015. doi:10.1021/ct800526s

Ufimtsev, I. S., and Martinez, T. J. (2009b). Quantum Chemistry on Graphical Processing Units. 3. Analytical Energy Gradients, Geometry Optimization, and First Principles Molecular Dynamics. *J. Chem. Theor. Comput.* 5 (10), 2619–2628. doi:10.1021/ct9003004

Wang, L.-P., Titov, A., McGibbon, R., Liu, F., Pande, V. S., and Martínez, T. J. (2014). Discovering Chemistry with an *Ab Initio* Nanoreactor. *Nat. Chem* 6, 1044–1048. doi:10.1038/nchem.2099

Watson, W. D. (1973). The Rate of Formation of Interstellar Molecules by Ion-Molecule Reactions. *ApJ* 183, L17–L20. doi:10.1086/181242

Zimmerman, P. M. (2013). Automated Discovery of Chemically Reasonable Elementary Reaction Steps. *J. Comput. Chem.* 34, 1385–1392. doi:10.1002/jcc.23271